

A Droplet in a Stationary Electric Field

Dirk Langemann

University of Rostock, department of mathematics, D-18051 Rostock, Germany

Abstract

Water droplets on insulating material influence strongly the aging process of the material. The shape of the droplets signifies the state of the aging material. The present paper discusses a procedure to calculate the droplet shape in an electric field generated by a constant voltage. A combined stationary solution of the droplet shape and the electric field is searched for. The typical shapes of the droplets are shown for several voltages. Special care is taken to the singularities of the electric field in the triple points.

Key words: stationary electric field, insulators, droplets, boundary value problem, corner points

1 Introduction

This investigation is initiated by the observation that water droplets on the surface of insulating material influence strongly the process of its aging. While aging the material loses its hydrophobic and insulating characteristics and hence its proper purpose, [3].

The present paper considers a simple droplet in a stationary electric field. The droplet lies on a solid support made of resin, and the electric field is generated by a voltage between two electrodes inside the resin. The acting forces and the droplet shape are determined. Note that the droplet shape feeds back to the electric field again.

Although in reality alternating current will be the standard application, it seems to be reasonable to investigate a stationary situation. On the one hand, the inertial effects inside the droplet and the inductional effects caused by the low frequency field are assumed to be rather small, [6]. On the other hand,

Email address: `lgm@alf.math.uni-rostock.de` (Dirk Langemann).

the stationary problem is already complex enough to be worth studied. An essential point is the feed-back of the droplet whose shape depends on the electric field, and influences the electric field again.

In Sec. 2, we will give an overview on the type of the problem and we will present a general iteration method. Sec. 3 deals with finding the shape of the droplet for a given outer force density caused by the electric field, and Sec. 4 works out the inverse problem to the preceding one. Both take special care to the situation in the edges of the droplet, the so-called triple points between the solid support, the droplet fluid and the air.

Finally, Sec. 5 presents the results for the two-dimensional problem. In particular the droplet shapes are given for different strengths of the electric field.

2 Problem set-up

We investigate a two-dimensional problem to study typical effects. In the respective three-dimensional problem, all quantities are constant in the direction vertical to the chosen intersection plane. Although this equivalence, we refer all quantities in a two-dimensional sense only.

The droplet is described by its upper boundary Γ which is given in polar coordinates with the origin O , i. e. $\Gamma = \{x_\Gamma = (r(\varphi) \cos \varphi, r(\varphi) \sin \varphi) ; \varphi \in [0, \pi]\}$. The angle φ serves as parameter of the points $x_\Gamma(\varphi)$ at the boundary. The droplet fluid is in fact water with the mass density $\delta = 1000 \text{ kgm}^{-3}$ and the surface traction $\alpha = 0.072 \text{ Nm}^{-1}$.

The electric field is generated by two electrodes in the support. The voltage between them is $2U$. The boundary of the electrodes is called Γ_1 .

The domain outside the droplet and outside the electrodes is called Ω . This domain is the support of the electric field, and the electric field depends on the droplet shape via the droplet boundary Γ , cf. Fig. 1. The points A and B are needed in Sec. 3.2 and 4.3.

The droplet itself and the electrodes are assumed to be free of electric field. Comparing the dielectricity $\varepsilon_{\text{H}_2\text{O}} = 81$ with $\varepsilon_1 = 1$ of the air and $\varepsilon_2 = 4$ of the solid support, the assumption seems to be reasonable.

Now, the electric field causes a concentration ρ_Γ of electric charge at the boundary Γ of the droplet. This results in a force density $p_e(\varphi) = p_e(x_\Gamma(\varphi))$ at Γ . Obviously, a similar force density acts at the boundaries of the electrodes but is not considered here.

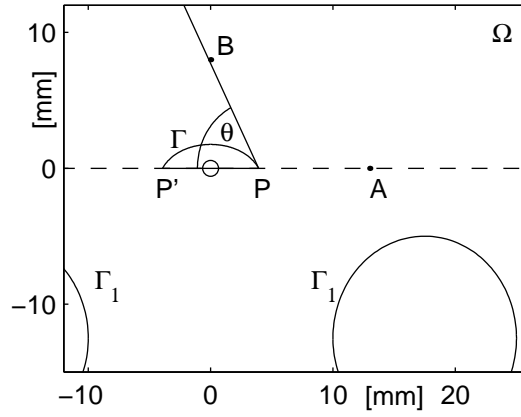


Fig. 1. Model set-up of the problem. The droplet lays in the centre on the surface of the solid support containing two electrodes.

Looking at the problem from a more abstract view-point, we remark two sub-problems. Finding r for a given p_e will be referred to as \mathcal{R} -problem, and finding p_e for a given r is called \mathcal{P} -problem. There are two operators \mathcal{R} and \mathcal{P} mapping a fixed force density p_e to a resulting r and vice versa, a given r to a force density p_e :

$$\mathcal{R} : p_e \rightarrow r \text{ and } \mathcal{P} : r \rightarrow p_e .$$

while solving the problem of finding the stationary shape of the droplet in the electric field, we are searching a fixed point of the combined operator $\mathcal{R}\mathcal{P}$, i. e. $r_{fix} = \mathcal{R}\mathcal{P}r_{fix}$.

To separate both problems we state the iteration

$$r^{(i+1)} = \omega \mathcal{R}\mathcal{P}r^{(i)} + (1 - \omega)r^{(i)} \quad (1)$$

with the relaxation parameter ω . Basing on the physical background and thus the natural existence of a stable stationary solution, we hope that

$$\lim_{i \rightarrow \infty} r^{(i)} = r_{fix} \text{ (point-wise)} \quad (2)$$

at least for suitable ω . Knowing that an analytical prove will be hard work, we will see by testing that the convergence (2) holds.

3 The \mathcal{R} -problem

This section deals with the determination of the shape of the droplet under the influence of a given normal force density p_e acting on its upper boundary Γ .

3.1 The acting force densities

The following pressures are acting in a point $x_\Gamma = (r(\varphi) \cos \varphi, r(\varphi) \sin \varphi)$ with $\varphi \in (0, \pi)$ at the upper boundary of the droplet in the direction of the outer normal n on Γ :

- (1) The curved boundary produces a curvature pressure p_k resulting from the surface traction, s. [1], which is

$$p_k(\varphi) = -\alpha \cdot \kappa(\varphi) \quad \text{with} \quad \kappa(\varphi) = \frac{r(\varphi)^2 + 2r'(\varphi)^2 - r(\varphi)r''(\varphi)}{(r(\varphi)^2 + r'(\varphi)^2)^{\frac{3}{2}}}. \quad (3)$$

- (2) The pressure inside the droplet depending on the depth of the water is

$$p_h(\varphi) = \delta g(h - r(\varphi) \sin \varphi) \quad \text{with} \quad h = \max_{\varphi \in [0, \pi]} r(\varphi) \sin \varphi. \quad (4)$$

Here δ denotes the mass density of the droplet fluid and g is the gravity acceleration.

- (3) Under the acting pressures the droplet changes slightly its volume. Therefore, we have a pressure resulting in the volume dilatation

$$p_0 = \left(\frac{V}{V_r} - 1 \right) p_{air} \quad \text{with} \quad V_r = \frac{1}{2} \int_0^\pi r(\varphi)^2 d\varphi \quad (5)$$

and an assumed volume V of the undeformed droplet fluid under the air pressure p_{air} . Eq. (5) replaces a possible condition of incompressibility in the present formalism of equilibrated forces.

Summarizing Eqs. (3-5) and the outer force density p_e , it holds

$$0 = p_k(\varphi) + p_h(\varphi) + p_0(\varphi) + p_e(\varphi) \quad (6)$$

in every point $x_\Gamma(\varphi)$ with $\varphi \in (0, \pi)$ except in the corners $P = x_\Gamma(0)$ and $P' = x_\Gamma(\pi)$.

3.2 The behaviour in the corner points

In the corner P the surface traction α acts between the fluid and the air in the direction PB and the boundary traction $\alpha_{1,2}$ acts between the solid support and the fluid in the direction PA . The boundary traction between the solid and the air is assumed to be negligible.

The adhesion force may behave like a Lagrangian multiplier normal to the

surface of the solid support and the angle $\vartheta = \angle BPO$ is given by

$$\cos \vartheta \cdot |\alpha| = \alpha_{1,2} \cdot \tau \quad (7)$$

where $\tau \| PA$ is of length 1, [1]. Note, that α and $\alpha_{1,2}$ are forces instead of being force densities. The angle ϑ can only be changed by additional forces entering Eq. (7). But they do not in the actual problem, as will be shown in Sec. 4.3.

Thus, we get the boundary conditions in the corners P and P'

$$\tan \vartheta \cdot r'(0) + r(0) = 0 \quad \text{and} \quad \tan \vartheta \cdot r'(\pi) - r(\pi) = 0. \quad (8)$$

In the examples of Sec. 5, $\vartheta = 1.1$ is used.

3.3 Numerical treatment

Eq. (6) with the boundary conditions (8) is a non-linear boundary value problem for $r(\varphi)$ on $\varphi \in [0, \pi]$. It can be handled by introducing an auxiliary time t and solving instead the time-dependent problem

$$\frac{\partial}{\partial t} r(\varphi, t) = p_k(\varphi) + p_h(\varphi) + p_0(\varphi) + p_e(\varphi), \quad (9)$$

$$\frac{\partial}{\partial t} r(0, t) = k[\tan \vartheta \cdot r'(0, t) + r(0, t)] \quad \text{and} \quad \frac{\partial}{\partial t} r(\pi, t) = -k[\tan \vartheta \cdot r'(\pi, t) - r(\pi, t)] \quad (10)$$

where $r'(\cdot, t)$ denotes the derivative with respect to the first parameter and k is a suitable amplification factor, e. g. $k = \pi \frac{\alpha}{2V}$.

The solution $r(\varphi, t)$ converges with $t \rightarrow \infty$ to a time-constant radius which fulfils Eqs. (6) and (8). The convergences follows from the fact that the acting force densities would drive a droplet of a very viscose fluid to its stationary shape. Here a time-constant radius is reached is less than $1 \cdot 10^{-4}$ s, cf. Fig. 2.

Eqs. (9-10) can be discretized over φ and solved by standard methods for stiff ordinary differential equations, [2], like e. g. `ode15s` in `Matlab`. In the examples of Sec. 5 the interval $[0, \pi]$ was discretized into 200 equidistant grid points.

4 The \mathcal{P} -problem

This section deals with the determination of the electric potential $\Phi(x)$ in the domain Ω and thus in whole the plane. Having once $\Phi(x)$, we will find the

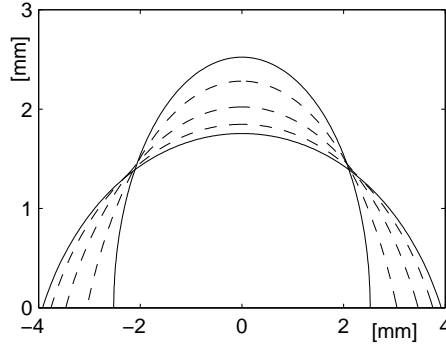


Fig. 2. Evolution of the radius in the time-dependent problem starting with $r(\varphi) = \text{const.}$ and setting $p_e \equiv 0$. The solid lines mark the initial and final state of the droplet. The dashed lines give the radius at the auxiliary time-instants $t = 2 \cdot 10^{-5} \text{ s}$, $t = 6 \cdot 10^{-5} \text{ s}$ and $t = 10 \cdot 10^{-5} \text{ s}$ (from above).

resulting force density p_e .

4.1 The electric potential

The electric potential $\Phi(x)$ coincides at the electrodes and their boundaries Γ_1 with the voltage U resp. $-U$. The boundary of the droplet Γ is an iso-potential line and cause of symmetry, it holds $\Phi(x_\Gamma) = 0$ there. The domain Ω outside the electrodes and the droplet is free of electric charge.

We regard $\Phi(x)$ in the right half-plane. Inside the electrode and inside the droplet, it is constant. Inside Ω we get the boundary value problem, [4]

$$\begin{aligned} -\nabla \cdot (\varepsilon(x) \nabla \Phi(x)) &= 0 \quad \text{in } x \in \Omega, \\ \Phi(x) &= 0 \quad \text{on } x \in \partial\Omega \setminus \Gamma_1, \\ \Phi(x) &= U \quad \text{on } x \in \Gamma_1. \end{aligned} \tag{11}$$

Using Cartesian co-ordinates with origin O and $x = (x_1, x_2)$ the dielectricity is

$$\varepsilon(x) = \begin{cases} \varepsilon_1 & x \in \Omega, \quad x_2 \geq 0, \\ \varepsilon_2 & x \in \Omega, \quad x_2 < 0. \end{cases} \tag{12}$$

In Eq. (12), the values of the dielectricity at the surface of the solid support are arbitrary.

Now, the electric field and the displacement are given by

$$E(x) = -\nabla \Phi(x) \quad \text{and} \quad D(x) = \varepsilon_0 \varepsilon(x) E(x).$$

The density ρ of electric charge is concentrated on the boundary of Ω , in

particular on the boundary Γ of the droplet. It vanishes in the environment of Γ outside Γ . Thus

$$\rho(x_\Gamma) = \nabla \cdot D(x_\Gamma) = -\varepsilon_0 \varepsilon_1 \left(\frac{\partial^2}{\partial n^2} \Phi(x_\Gamma) + \kappa(\varphi) \frac{\partial}{\partial n} \Phi(x_\Gamma) \right), \quad (13)$$

where n is still the outer normal of the droplet and thus the inner normal of the domain Ω at Γ .

Eq. (13) is obtained by expressing $-\nabla \cdot (\varepsilon(x) \nabla \Phi(x))$ in curvilinear co-ordinates and using the fact that the displacement D is constant inside the droplet.

Integration of Eq. (13) in normal direction over $[x_\Gamma - \nu n, x_\Gamma + \nu n]$ with a small $\nu > 0$ provides the density ρ_Γ of electric charge on the boundary of the droplet. That is

$$\rho_\Gamma(x_\Gamma) = \int_{-\nu}^{\nu} \rho(x_\Gamma + \sigma n) d\sigma = -\varepsilon_0 \varepsilon_1 \frac{\partial}{\partial n} \Phi(x_\Gamma).$$

Thus, the force density p_e acting on the boundary of the droplet is

$$p_e(\varphi) = \rho_\Gamma(x_\Gamma(\varphi)) E(x_\Gamma(\varphi)) = \varepsilon_0 \varepsilon_1 \left(\frac{\partial}{\partial n} \Phi(x_\Gamma(\varphi)) \right)^2. \quad (14)$$

4.2 Numerical handling

Using the symmetry, we consider Eq. (11) only in the right half-plane. The half-plane is restricted by a rectangle. The error due to the restriction is regarded to be small because of the local character of any disturbances of the electric field.

The boundary value problem (11) with its Dirichlet boundary conditions is solved by standard finite elements on a triangulation, cf. Fig. 3. The triangulation is refined near the boundary of the droplet. It is created once in a pre-processing and adapted to each present shape of the droplet.

In the present examples a triangulation with 6011 points and 11621 triangles was used. This leads to 48 triangles sharing a side with the discretized boundary of the droplet. Solving the resulting system of linear equations is done by standard procedure for sparse matrices without any additional effort. The solution was checked and regarded to be just fine.

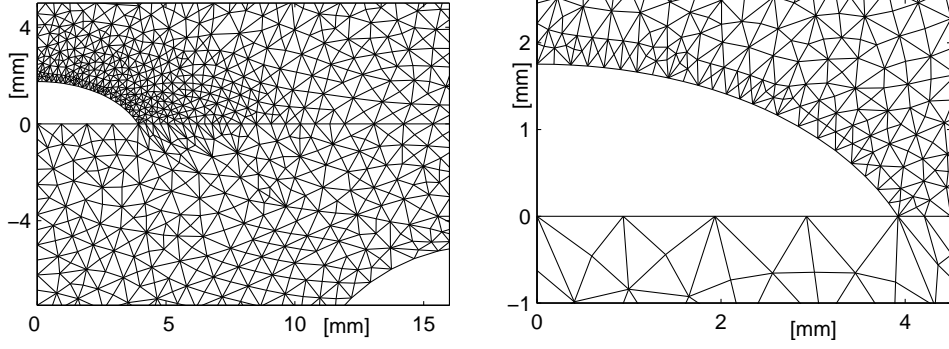


Fig. 3. Details of the triangulation. An electrode is remarkable at the righth bottom of the left figure. Both contain a droplet under the absence of an electric field.

4.3 The electric field close to the corners

We regard the electric potential Φ near the corner P of the droplet and use polar co-ordinates (s, ψ) with origin P and the $\psi = 0$ at PA .

Inside the angle $\angle BPA$ the electric potential has the expansion

$$\Phi^{(1)}(s, \psi) = \sum_{i=1}^{\infty} b_i^{(1)} s^{a_i^{(1)}} \sin(a_i^{(1)}(\pi - \vartheta - \psi)). \quad (15)$$

In Eq. (15) $b_i^{(1)}$ and $a_i^{(1)}$ are suitable coefficients with $a_{i+1}^{(1)} > a_i^{(1)}$ for all i , [5]. Respectively, inside $\angle OPA$ the expansion may be

$$\Phi^{(2)}(s, \psi) = \sum_{i=1}^{\infty} b_i^{(2)} s^{a_i^{(2)}} \sin(a_i^{(2)}(\psi + \pi)). \quad (16)$$

Now, on the line PA holds

$$\Phi^{(1)}(s, 0) = \Phi^{(2)}(s, 0) \quad \text{and} \quad \varepsilon_1 \frac{\partial}{\partial \psi} \Phi^{(1)}(s, 0) = \varepsilon_2 \frac{\partial}{\partial \psi} \Phi^{(2)}(s, 0). \quad (17)$$

The leading terms in the expansions (15-16) determine the behaviour of Φ close to the corner P and hence the singularity of E there.

Thus, the comparison of the first terms in Eq. (17) yield with $b = b_1^{(2)}/b_1^{(1)}$

$$s^{a_1^{(1)}} \sin(a_1^{(1)}(\pi - \vartheta)) = b s^{a_1^{(2)}} \sin(a_1^{(2)}\pi) \quad \text{and} \quad (18)$$

$$-\varepsilon_1 a_1^{(1)} s^{a_1^{(1)}} \cos(a_1^{(1)}(\pi - \vartheta)) = \varepsilon_2 b a_1^{(2)} s^{a_1^{(2)}} \cos(a_1^{(2)}\pi). \quad (19)$$

Eq. (18-19) hold for $s \rightarrow 0$ and all other terms of Eqs. (15-16) are vanishing faster than the first one. Thus, it is set $a = a_1^{(1)} = a_1^{(2)}$. Eq. (18) simplifies to

$$\sin(a(\pi - \vartheta)) = b \sin(a\pi) \quad \text{and} \quad -\varepsilon_1 \cos(a(\pi - \vartheta)) = b \varepsilon_2 \cos(a\pi).$$

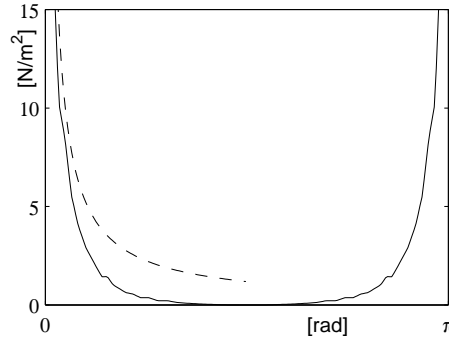


Fig. 4. Force density $p_e(\varphi)$ resulting from an electric field generated by $U = 8$ kV. For comparison, the dashed line shows $c\varphi^{2(a-1)}$.

A simple calculation shows that the minimal a fulfils $\frac{1}{2} < a < 1$. In fact, for $\vartheta = 1.1$ the minimal a we get, is $a = 0.54$.

The electric potential behaves like $\Phi^{(1)}(s, \psi) \sim s^a \sin(a(\pi - \vartheta - \psi))$ for $s \rightarrow 0$. It follows that

$$p_e(\varphi) \sim \left(\frac{1}{\varphi} \frac{\partial}{\partial \psi} \Phi^{(1)}(r(\varphi)\varphi, \pi - \vartheta) \right)^2 \sim \varphi^{2(a-1)} \quad \text{for } \varphi \rightarrow 0$$

what can be used for checking the numerical solution, cf. Fig. 4.

On the other hand, the density of electric charge in the corner P with $x_P = x_\Gamma(0)$ is

$$\rho(x_P) = -\Delta\Phi(x_P) = -\varepsilon_0 \lim_{\Theta \rightarrow P} \int_{\partial\Theta} \varepsilon(x) \nabla\Phi(x) \cdot n_\Theta(x) dx = 0 \quad (20)$$

where Θ is a circle around P contracting to P . Its outer normal is $n_\Theta(x)$. Eq. (20) follows from $\nabla\Phi(s, \psi) \sim s^{a-1}$ and $dx = sd\psi$. It shows that there is no essential concentration of electric charge in the corner and thus there is no additional force to disturb Eq. (7).

5 Results

The iteration (1) works rather fast. For low voltages $U < 5$ kV, it needs about five steps with $\omega = 1$ to find a fixed-point of the operator \mathcal{RP} in the range of machine accuracy.

Larger voltages require a smaller relaxation parameter and thus more steps. We have done calculations up to $U = 18$ kV where we have used $\omega = 0.15$ and needed about 20 steps.

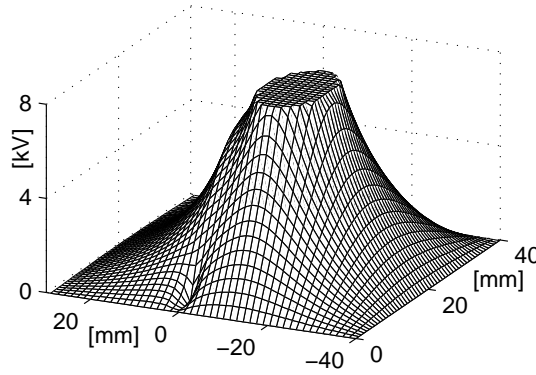


Fig. 5. The electric potential Φ in the case $U = 8$ kV. It vanishes inside the droplet in front, and it is constant inside the electrode. The refraction at the interface of the solid support and the air is remarkable.

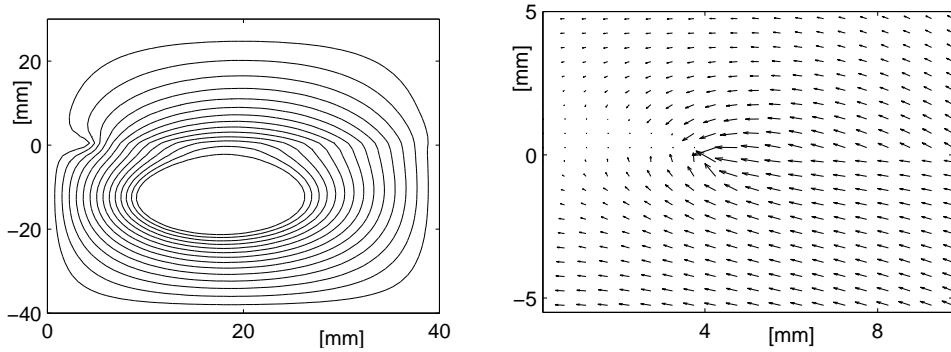


Fig. 6. Left : Levels from $\Phi = 0.5$ kV up to $\Phi = 7$ kV in the case $U = 8$ kV. Refraction of the level lines is visible at $x_2 = 0$. Right : The electric field E near the corner P .

On a 400 MHz-workstation, one iteration step takes about 3 min. It contains solving the discretized partial boundary value problem (11) on the preprocessed triangulation, described in Sec. 4.2, calculating p_e , solving a stiff ordinary boundary value problem (6) with the boundary conditions (8) to find the new $r^{(i+1)}(\varphi)$ and the adaptation of the triangulation to the new intermediate droplet shape $r^{(i+1)}(\varphi)$.

A typical electric potential Φ is presented in Fig. 5. The belonging electric field E is shown by its level lines in Fig. 6. Further, it is given near the droplet, in particular near the corner point P . The resulting force density p_e on Γ was already referred to in Fig. 4.

Let us remark, that the \mathcal{P} -problem is linear in U . But this linearity does not continue to the whole problem due to the different shapes of the droplet. Nevertheless, the example given here represents the qualitative behaviour of electric potentials for other voltages, too.

Finally, Fig. 7 shows droplet shapes for different voltages. The droplets are be-

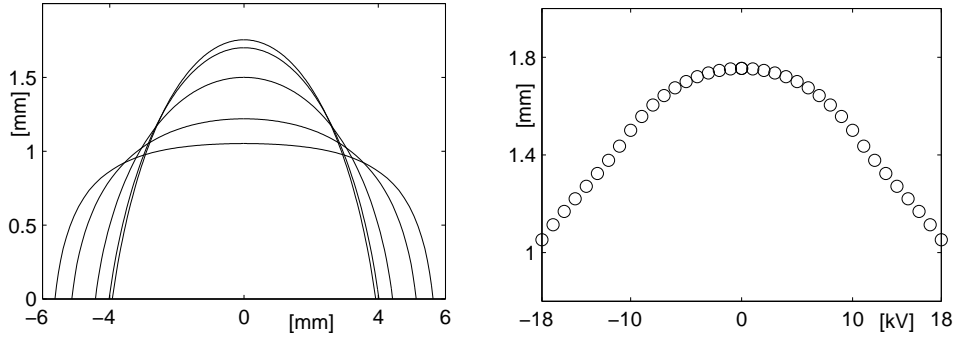


Fig. 7. Left : Droplet shapes for $U = 0$ kV, $U = 5$ kV, $U = 10$ kV, $U = 15$ kV and $U = 18$ kV (from above). Right : Droplet heights depending on the voltage U .

coming wider and flatter with increasing voltage. For low voltages, the change of width and height of the droplets is relatively small. It becomes more remarkable for $U > 5$ kV, and the the shape of the droplet resembles a plateau for $U \approx 18$ kV. If the voltage is increased further, the droplet will loose connectivity after a short interval where it has a local minimum of height at $x_1 = 0$.

The right plot of Fig. 7 presents the heights of the droplets depending on the applied voltages U . The height does not depend on the sign of the voltage, comp. Eq. (14). Thus, assuming all inertial and inductional effects to be small enough, the droplets oscillate with twice the frequency of the applied alternating current.

6 Conclusion

The stated problem of determining the shape of a water droplet in a stationary electric field was described as a fixed-point problem and solved by a Banach-like iteration. It contains two sub-problems.

The first of them consists in finding the droplet shape for a given outer force density acting at the boundary of the droplet. It was solved by calculating an evolution problem for the radius tending to a stationary solution.

The second sub-problem to compute the electric field and hence to outer acting force density, was handled by finite elements on an adapted triangulation. It works by standard procedures without any numerical sophistication.

Special care has to be devoted the behaviour in the triple points. The behaviour of the electric potential close to these corner points were investigated analytically. The result was checked with numerical calculations.

We resume to have a suitable procedure to handle the two-dimensional problem of a droplet in a stationary electric field. It can be extended to the essentially three-dimensional problem of a droplet on a solid support in a straightforward manner.

The extension to a time-dependent solution with an alternating voltage involves new difficulties of a completely different kind like flux inside the droplet fluid, inertial effects, induced currents in the fluid and so on.

References

- [1] E. Grimsehl, Lehrbuch der Physik, Band 1, (Course on theoretical physics, volume 1), Teubner, Leipzig (1987)
- [2] E. Hairer, G. Wanner, Solving Ordinary Differential Equations 2, Stiff and Differential-Algebraic Problems, Springer, Berlin (1991)
- [3] S. Keim, D. König, Study of the Behavior of Droplets on Polymeric Surfaces under the Influence of an Applied electrical Field, IEEE Conference on Electrical Insulation and Dielectric Phenomena, Austin, October 17-20, pp. 707-710 (1999)
- [4] L. D. Landau, E. M. Lifschitz, The classical theory of fields, Butterworth, Washington DC (1997)
- [5] M. Renardy, R. C. Rogers, An Introduction to Partial Differential Equations, Springer, New York (1992)
- [6] U. van. Rienen, M. Clemens, T. Wendland, *Simulation of Low-Frequency Fields on Insulators with Light Contaminations*. IEEE Transactions on Magnetics, Vol. **32**, No. 3, pp. 816-819 (1996)